Journal of Interfaces, Thin films, and Low dimensional systems 3 (1) Summer and Autumn (2019) 203-210

DFT study of Benzene, Coronene and Circumcoronene as zigzag graphene quantum dots

Scientific research paper

Hamed Asadi[1*], Kazem Zhour[1], and Ahmad Zavartorbati[2]

[1]*Solid state Physics Department, Physics Faculty, K.N. Toosi University of Technology, Tehran, I.R. Iran*

[2]*Power and Electronics Department, Farabi University of Science & Technology, Tehran, I.R. Iran*

ARTICLE INFO

Article history:
Received 5 April 2020
Revised 17 May 2020
Accepted 9 June 2020
Available online 25 July 2020

Keywords:
DFT
Quantum dots
Graphene
Raman Spectroscopy
Benzene
Coronene
Circumcoronene

ABSTRACT

Theoretically, graphene quantum dot (GQD) has proved to feature in several important applications during recent decades. Generally, quantum dot, which is of nano-scale size is comparable to the size of atoms and molecules, having different properties from the bulk of the same materials. In Nano scales, the electrical, optical, thermodynamic, and mechanical properties of samples are directly related to the number of atoms constituting the sample, regarding size and shape (type of edge, forms, and dimensions). In this paper three different structures of GQDs with zigzag edges (Benzene, Coronene, and Circumcoronene) have been considered and simulated using the DFT theory by applying PBE functional in order to extract the thermal energy, electronic energy, heat capacity, polarizability, and entropy of each structure. The modification of each property with respect to the number of atoms in the GQD are investigated, linear and nonlinear variations of these properties with respect to the atom number are observed. Comparative study of Raman spectroscopy between PBE and B3LYP functionals is studied for each size of the considered GQDs. Also, revolution of the G peak in each case has been separately investigated. All calculations are done by using the Gaussian 09W software package based on 3-21G Gaussian basis sets.

1 Introduction

Graphene is one of the most promising materials under study in our decade due its global potential and ability of improving numerous fields and applications which can take human life to another level of civilization. Many researchers suppose that if the previous century was the age of plastics (silicone), this century seems to become the age of graphene [1]. Since 2004, the number of graphene-related publications has substantially increased, where the number of published articles related to graphene in journals exceed 15000 in 2014 [2]. Graphene quantum dots and their derivatives grab more attention because of their high free electron density, extraordinary conductivity, small size, and high surface-to-volume ratio which affects their electronic, optical, and mechanical properties [3].

*Corresponding author.
Email address: Hasadi@Mail.kntu.ac.ir
DOI: 10.22051/jitl.2020.30897.1036

Generally, properties of quantum dots are different from large structures made of the same materials. Indeed, they have the potential of tunability which leads to a wide diversity of applications, such as, semiconductor electronic, light emitting diodes (LED), quantum computing, solar cells, medical usages, bio-imaging, cancer therapy, and plasmonics, etc. Moreover, the ultra-high carrier mobility of graphene and its linear dispersion band structure, prepare it for optoelectronic applications [4].

Armchair and zigzag edge terminations are the most stable quantum dots between all different shapes of graphene honeycomb lattice. In this work, concentrate is put on studying zigzag edges quantum dots due to the appearance of strongly localized edge states, where this type of edge termination significantly affects the energy spectra and consequently their optical and electrical properties [2–4]. A simulation study showed that the optical properties of graphene quantum dots depends on their structure, shape, and size [5].

In this paper, zigzag graphene quantum dots (ZGQDs) have been studied while influence on their sizes by considering the number of loops from the center of the first hallow site of hexagonal on several properties of ZGQDs have been investigated. Three ZGQDs were selected; 1-loop ZGQD1 consists of 6 carbon atoms and 6 hydrogen atoms which is the benzene molecule, 2-loop ZGQD2 with 7 hexagons which consisted of 24 carbon atoms and 12 hydrogen atoms known as the coronene molecule, and finally, 3-loop ZGQD3 constructed by 19 hexagons, 54 carbon atoms constrained by 18 hydrogen so-called circumcoronene (

Figure 1). Many previous studies have considered these structures and investigated their properties theoretically using different methods [6–11].

2 Method

The calculations in this work have been done by the DFT theory using two famous functionals for exchange correlation energy approximations; the generalized gradient approximation PBE functional (Perdew, Burke and Ernzerhof functional) [12] and the hybrid B3LYP functional (Becke's gradient-corrected exchange correlation in conjunction with the Lee–Yang–Parr correlation functional with three parameters) [13,14]. The Gaussian 09W software package [15], which is based on Gaussian basis sets together with the GaussView 05 visualization software are used to accomplish this study. In our case, 3-21G Gaussian basis sets is applied for all the performed calculations, in order to extract the thermal and electronic properties such as electronic energy, heat capacity, polarizability, entropy, and Raman spectra to each of the considered structures of ZQGDs. First of all, quantum dots have been optimized to obtain the optimum bond length of each structure. Next and calculation has been done to extract optical, thermal, and electrical

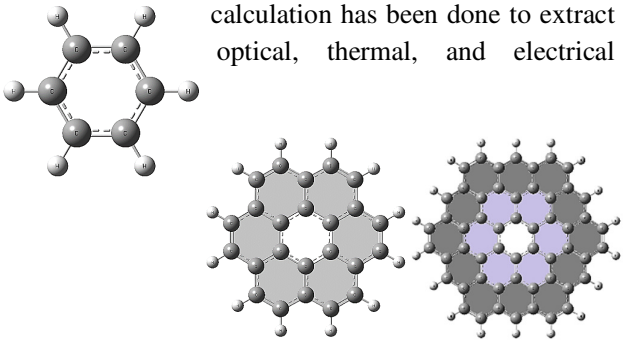

Figure 1. Left panel, graphene quantum dots consist of one hexagonal (Benzene). Middle panel, two loops of hexagons (Coronene). Right panel, three loops of hexagons (Circumcoronene).

3 Results

First of all, the bond lengths at the edges of each structure have been measured after the optimization and order according to Table 1. The bond locations in each structure are labeled in Figure 1.

Table 1: Optimized bond lengths at the counter of each considered ZGQD

Structure	Bond symbol	Bond number	Bond length B3LYP	Bond length PBE
ZGQD1	C=C	(1)	1.397	1.405
	C−H	(2)	1.084	1.093
ZGQD2	C=C	(1)	1.426	1.431
	C=C	(2)	1.372	1.382
	C−H	(3)	1.085	1.094
ZGQD3	C=C	(1)	1.402	1.410
	C=C	(2)	1.440	1.443
	C=C	(3)	1.362	1.374
	C−H	(4)	1.085	1.095
	C−H	(5)	1.085	1.094

The thermal and electrical properties of the GQDs are presented in Table 2, as the graphical representations of these results are shown in Figures 2 and 3.

Table 2: Different calculated properties of each considered ZGQD

Number of atoms	Polarizability (a.u)	Electronic Energy (Hartree)	E (Thermal) (kcal/mol.K)
12	51.31	-230.66	64.83
36	261.14	-915.66	180.48
72	387.16	-2054.99	345.15

Number of atoms	Heat Capacity (cal/mol.K)	Entropy (S) (cal/mol.K)
12	17.43	64.28
36	66.31	114.43
72	141.61	178.48

As shown in Figures 2 and 3, the polarizability and the entropy are not linear functions with respect to the number of atoms, while the electronic energy, thermal energy, and heat capacity vary linearly with the number of atoms. The main source of polarization is the transfer of charge between hydrogen and carbon atoms at the edge of the structure which depends on the ratio of number of carbon atoms to that of hydrogen atoms. The polarizability, as a function of the number of atoms and temperature was well fitted as an exponential function:

$$P = A - B\exp\left(-\alpha\frac{N}{T}\right),$$

$$P = 451.3 - 576.8\exp\left(-\frac{N}{23.78}\right), \qquad (11)$$

where α, t, and T are the absorption coefficient, thickness, and transmittance of the film, respectively. By using interpolation, $\alpha = \frac{T}{23.78}$. At room temperature (293 K) we have α ~12.3. It can be noticed that the slope of the curve of polarizability decreases with the increase of the number of atoms in the considered structure, which means that the saturation can be reached for bigger structures. In other words, by increasing the size, the variation of the polarizability will decrease, while for bigger structures, the change in polarizability will be small.

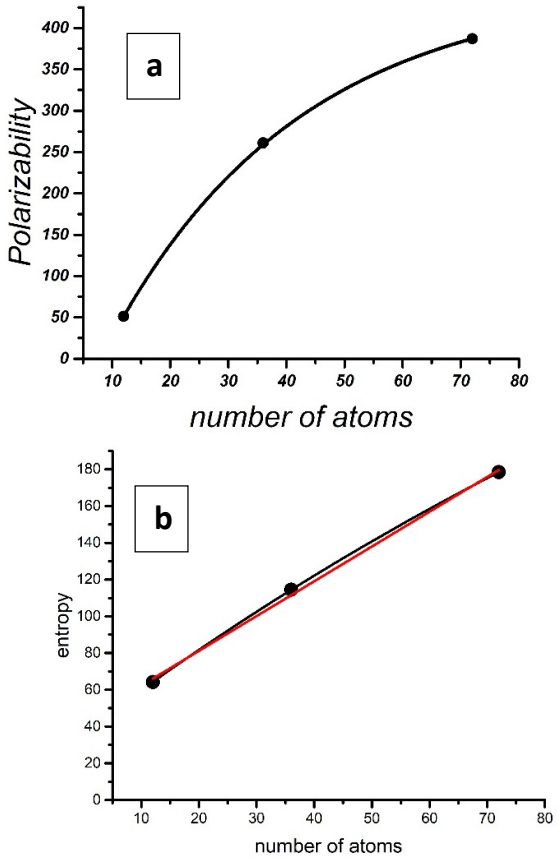

Figure 2. Polarizability (panel a) and entropy (panel b) as a function of number of atoms. The red line in panel b represents the fitted straight line.

Similarly, for the entropy, Eq. (2) can be obtained from the curve of Figure 2b for small number of atoms. The obtained result suggests that the entropy and its configurations will be rising exponentially with respect to the number of atoms. Consequently, by increasing the number of atoms, disordering of the systems increases as it is predictable by

$$\Omega = -443 + 480\exp\left(-\frac{N}{32.78}\right). \qquad (2)$$

The total energy is defined as the energy due to the contributions of the atoms, hence, in small size without overlapping the orbital, energy changes directly with respect to enhancing number of atoms [16].

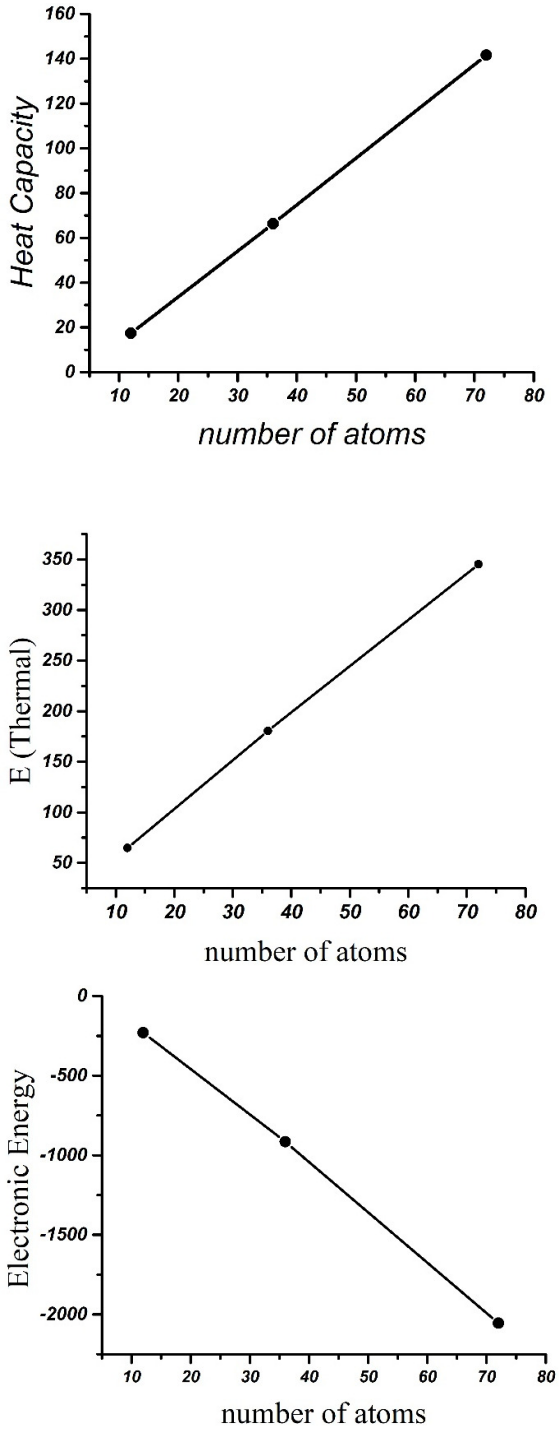

Figure 3. Heat capacity (top panel), thermal energy (middle panel), and electronic energy (bottom panel) as a function of the number of atoms in the structure.

On the other hand, The Debye temperature of materials and melting temperature have a specific relation that has been previously studied [17] as others follow this model for nano-scale materials [16,18] as

$$\theta_D \propto \left(\frac{T}{mV^{\frac{2}{3}}}\right)^{\frac{1}{2}}, \quad (3)$$

where m, V, T, and θ_D are the molecular mass, volume per atom, temperature, and Debye temperature, respectively. The relation between the specific heat "C_v" and Debye temperature is expressed as

$$C_v \propto \frac{1}{\theta_D^2}, \quad (4)$$

According to Eqs. (3) and (4) one can deduce that C_v is proportional to T as

$$C_v \propto T. \quad (5)$$

In another study, the linear relation between temperature and atom number has been investigated [19]. Accordingly, the thermal energy of atoms has a linear relation with the number of atoms. Figure (3) has the reasonable response for such manner.

The variation of heat capacity and thermal energy as a function of size in nano-scale structures has been previously investigated. The heat capacity and thermal energy in small atoms changes due to the number of atoms. Thermal energy in small atoms is a linear function as it is predictable. Every atom has its specific energy which causes the linear increase of the thermal energy with the increase of the number of atoms. But as the graphene sheet gets wider, the interaction between those atoms increases so that the energy reaches saturation. As the dimensions of semiconducting particles (such as quantum dots) decreases, the sizes of the particles become comparable to the size of the electron-hole distance which is known as the Bohr radius. This radius for graphene and graphene oxide is in order of 0.529 Å [20]. In such a size, the overlapping is much smaller than that in wide sheets. Obviously, for wide spread sheets, the overlapping will increase, and a nonlinear function will appear.

In the following, Raman spectroscopy of ZGQDs will be investigated. Many previous studies have focused on calculating the Raman spectroscopy of different types of GQDs theoretically and experimentally [21–23].

Raman spectroscopy of graphene is characterized by three essential peaks, namely, G, D. and 2D. The G peak is at about 1580 cm^{-1}, and it is due to the doubly degenerate zone center E_{2g} mode of oscillation at Γ point [24], see Figure 4a and 4b. The D peak appears at approximately 1350 cm^{-1} while the 2D band, also called as the G' band, is the second harmonic of the D band that peaks at approximately 2700 cm^{-1}. The D and 2D peaks are caused by the A_{1u} vibration mode of the graphene lattice [25,26].

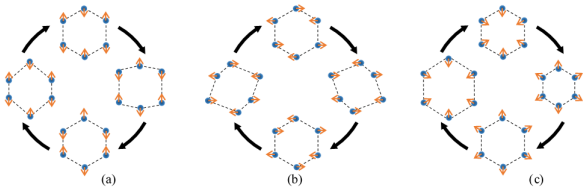

Figure 4. The doubly degenerate zone center E_{2g} modes of oscillation are presented in the left and middle panels. A_{1g} modes of oscillation for one loop of graphene sheet are presented in the right panel.

The Raman spectroscopy of ZGQD1, ZGQD2, and ZGQD3 are respectively shown in Figures 5, 6, and 7.

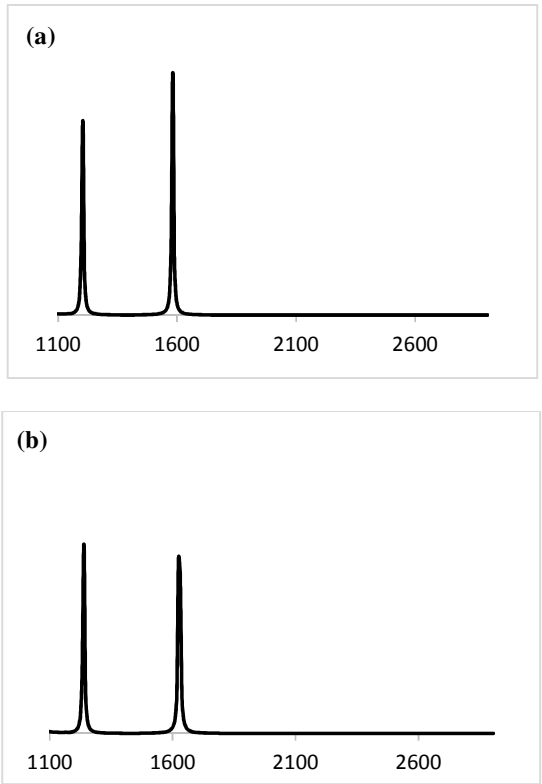

Figure 5. Raman spectroscopy of ZGQD1 based on (a) PBPBPE potential (b) B3LYP potential

The essential peak for each GQD is represented in Tables 3, 4, and 5 respectively.

Table 3. Essential peak of ZGQD1 between 1100 cm^{-1} and 2900 cm^{-1} with the mode of oscillation related to each peak.

PBE		
Frequency	Intensity	Vibration Mode
1224	8.9	C-H bending "ν_2"
1581	11.5	E_{2g}
B3LYP		
Frequency	Intensity	Vibration Mode
1237	8.1	C-H bending "ν_2"
1627	12.8	E_{2g}

From the spectroscopies of Figure 5, it can be noted that the G peak of the Raman spectroscopy of ZGQD1 appears at 1581 cm^{-1} in the case of PBE which is equal to the value of wide spared graphene sheet. But for B3LYP, the G peak appears at 1627 cm^{-1} (Figure 5).

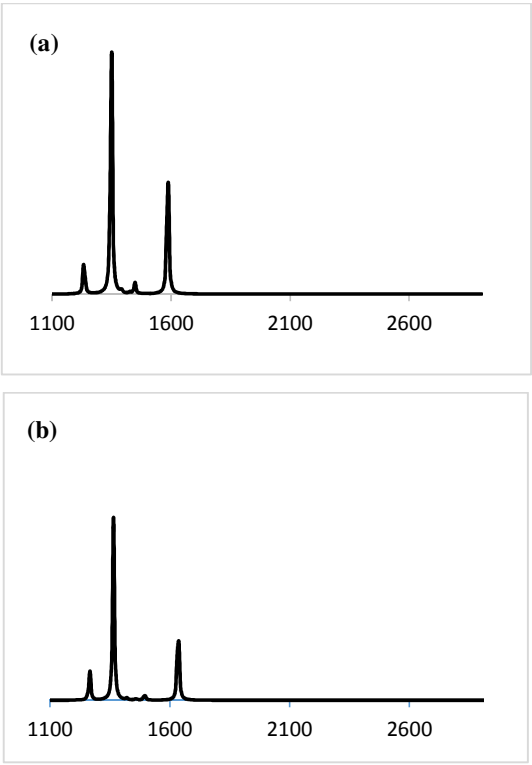

Figure 6. Raman spectroscopy of ZGQD2 Based on PBE potential (panel a) and B3LYP potential (panel b).

The peak at 1202 cm^{-1} for PBE and 1238 cm^{-1} for RB3LYP refers to the CH bend mode of oscillation. Such peaks do not appear in the case of wide spread graphene. The results of PBE are in good agreement with the frequencies of Raman spectroscopy of

Benzene given by the NIST Standard Reference Data [27], while the values given by B3LYP are not, especially for the C-H bending band frequency.

In the case of ZGQD2, the total number of peaks increases for both functionals. A large peak appears at 1349 cm^{-1} for PBE and at 1365 cm^{-1} for B3LYP. These peaks are D band that have the same frequency of that of graphene in the case of PBE while shifted approximately 15 cm^{-1} in the case of B3LYP. The C-H bending peak at 1233 cm^{-1} and 1266 cm^{-1} for PBE and B3LYP respectively becomes relatively very small in ZGQD2 with respect to the other peaks. The 2D band is still missing in the Raman spectroscopy of ZGQD2. The other weak peaks, due to their negligible intensities relative to other peaks, are not mentioned.

Table 4: Essential peak of ZGQD2 between 1100 cm^{-1} and 2900 cm^{-1} and the mode of oscillation related to each peak

PBE		
Frequency	Intensity	Vibration Mode
1233	91	C-H bending "ν_2"
1349	919	A_{1u}
1586	175	E_{2g}
B3LYP		
Frequency	Intensity	Vibration Mode
1266	165	C-H bending "ν_2"
1365	1043	A_{1u}
1634	194	E_{2g}

The number of peaks is significantly increased in the case of ZGQD3. The intensity of the peak corresponding to the C-H bending continues to decrease dramatically relatively to the other peaks as it is almost noticeable in both spectrometers. This decreasing can be referred to the dominance of the carbon atoms and their modes of vibrations. The D peak is divided into two peaks; one due to the A1u vibration of the edge loops with fixed central one at 1280 and 1295 cm-1 for PBE and B3LYP respectively, these frequencies are lower than those of ZGQD2. The other D peak appears at 1331 and 1346 cm-1 in each case and it is due to A1u vibration of the central loop. These frequencies are also slightly lower than the frequencies of the D band in the case ZGQD2. The G peak is divided into four peaks for PBE of frequencies 1531, 1561, 1578, and 1604 cm^{-1}. The same happens in the case of B3LYP but at frequencies 1576, 1609, 1628, and 1656 cm^{-1}. The last peak in both functionals represents the E_{2g} vibration of the edge loops where the central loop is fixed.

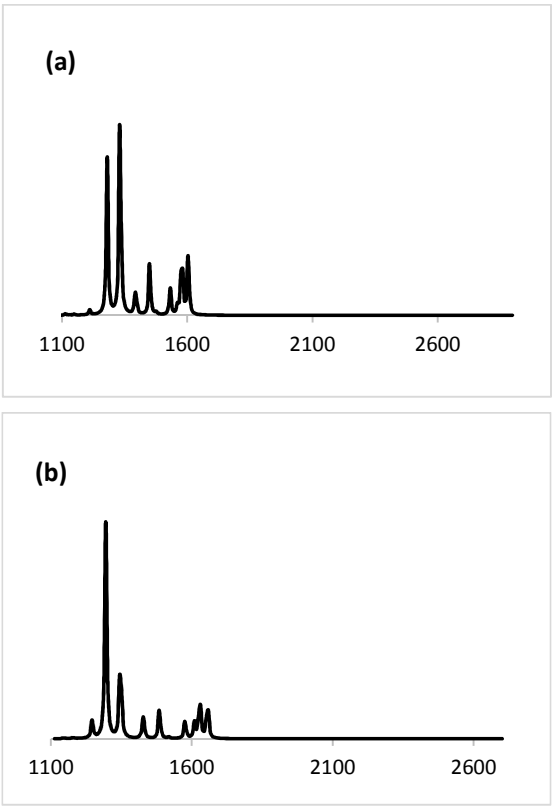

Figure 7. Raman spectroscopy of ZGQD3 Based on PBPBPE potential (panel a) and B3LYP potential (panel b).

Table 5. Essential peak of ZGQD3 between 1100 cm^{-1} and 2900 cm^{-1} and the mode of oscillation related to each peak.

PBE		
Frequency	Intensity	Vibration Mode
1210	91	C-H bending "ν_2"
1280	3056	A_{1u} with fixed central loop
1331	4488	A_{1u} of center
1395	475	E_{2g} with fixed central loop
1450	1122	A_{1u} of central loop
1531	291	E_{2g}
1561	82	E_{2g}
1578	779.7175	E_{2g}
1604	1322	E_{2g} with fixed central loop
B3LYP		
Frequency	Intensity	Vibration Mode
1246	505	C-H bending "ν_2"
1295	6178	A_{1u} with fixed central loop
1346	2733	A_{1u} of center
1429	563	E_{2g} with fixed central loop
1485	932	A_{1u} of central loop
1576	293	E_{2g}
1609	237	E_{2g}
1628	703	E_{2g}
1656	1297	E_{2g} with fixed central loop

The evaluation of the G peak in the three GQD structures is represented in Figure 8. It can be noticed that under both potentials, the G peak almost changes in the same manner but with a shifting in the values of the frequencies. In the case of ZGQD2, the G peak is slightly shifted towards higher frequencies with respect to that of ZGQD1 before dividing into four peaks with almost the same manner in both cases.

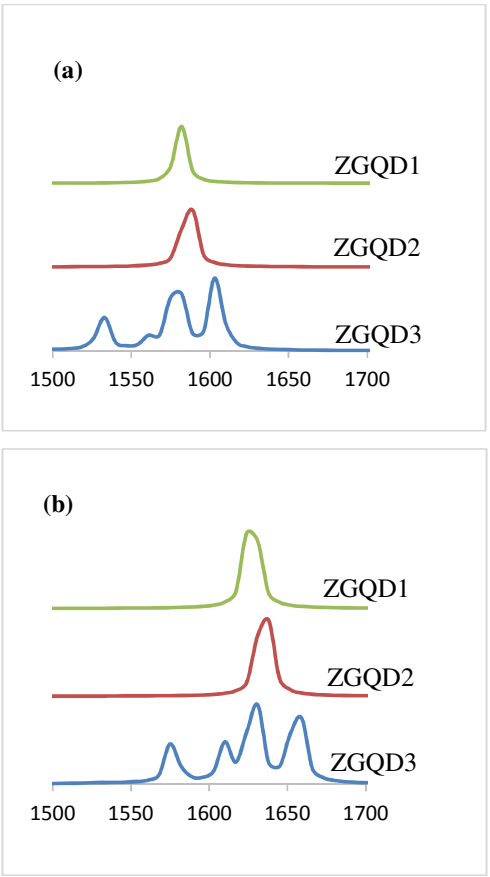

Figure 8. G peak of ZGQD1, ZGQD2, and ZGQD3 structures for the potential PBE (panel a) and B3LYP (panel b).

4 Conclusions

Benzene, coronene, and circumcoronene are considered as three different ZGQDs that have been theoretically studied using PBE and B3LYP functionals in a DFT simulation. The influence of the number of atoms of each structure on the thermal energy, electronic energy, heat capacity, polarizability, and entropy has been studied and compared. Thermal and electronic energy are linear functions of the number of atoms, likewise, the curve of heat capacity is a straight line. This is while, entropy and polarizability show nonlinear variation as a function of the number of atoms. The reason for each obtained result has been discussed. For entropy, the increasing of numbers of atoms in the sample leads to increment of the disordering exponentially. In the case of polarizability, the rate of the number of carbon atoms with respect to that of hydrogen atoms is the inherent reason of nonlinear variations. On the other hand, for total energy, the contribution of each atom plays the major role on the obtained result. Raman spectroscopy shows a good agreement with the preceding experimental and theoretical results of graphene. The two functionals (PBE and B3LYP) showed a little shifting of frequency between each other but with the same vibrational modes. Moreover, both methods indicate that the G peak is divided into 4 sub peaks in the case of ZGQD3. The GQDs provide interesting optoelectronic properties that can be tuned by controlling their size due to the quantum confinement. These extraordinary properties can be used in applications such as energy conversion bioanalytical sensors, optical qubits, and LEDs.

References

[1] Antonio H. Neto, Castro. "The carbon new age." Materials Today, **13** (2010) 12.

[2] S. Ahn et al. "Emerging analysis on the preparation and application of graphene by bibliometry." Journal of Material Sciences & Engineering, **4** (2015) 2169.

[3] Matthew J. Allen, Vincent C. Tung, and Richard B. Kaner. "Honeycomb carbon: a review of graphene." Chemical Reviews, **110** (2010) 132.

[4] Z. Jin et al., "Graphene, graphene quantum dots and their applications in optoelectronics." Current Opinion in Colloid & Interface Science, **20** (2015) 439.

[5] Y. Kobayashi et al., "Observation of zigzag and armchair edges of graphite using scanning tunneling microscopy and spectroscopy." Physical Review B, **71** (2005) 193406.

[6] M. Pykal et al., "Modelling of graphene functionalization." Physical Chemistry Chemical Physics, **18** (2016) 6351.

[7] J. Granatier et al. "The nature of the binding of Au, Ag, and Pd to benzene, coronene, and graphene: from benchmark CCSD (T) calculations to plane-wave DFT calculations." Journal of Chemical Theory and Computation, **7** (2011) 3743.

[8] Paulo V.C. Medeiros, Gueorgui Kostov Gueorguiev, and Sven Stafström. "Benzene, coronene, and circumcoronene adsorbed on gold, and a gold cluster adsorbed on graphene: Structural and electronic properties." Physical Review B, **85** (2012) 205423.

[9] M. Malček and M. Natalia DS Cordeiro. "A DFT and QTAIM study of the adsorption of organic molecules over the copper-doped coronene and circumcoronene." Physica E: Low-dimensional Systems and Nanostructures, **95** (2018) 59.

[10] Jennifer L. Weisman et al. "Time-dependent density functional theory calculations of large compact polycyclic aromatic hydrocarbon cations: implications for the diffuse interstellar bands." The Astrophysical Journal, **587** (2003) 256.

[11] E.M. Huff and P. Pulay. "A potential surface for the interaction between water and coronene as a model for a hydrophobic surface." Molecular Physics, **107** (2009) 1197.

[12] J.P. Perdew, B. Kieron, and M. Ernzerhof. "Generalized gradient approximation made simple." Physical Review Letters, **77** (1996) 3865.

[13] John P. Perdew, "Density-functional approximation for the correlation energy of the inhomogeneous electron gas." Physical Review B, **33** (1986) 8822.

[14] Becke, Axel D. "Density-functional exchange-energy approximation with correct asymptotic behavior." Physical review A, **38** (1988) 3098.

[15] M. J. E. A. Frisch et al. "Gaussian~ 09 Revision D. 01." (2014).

[16] M. Singh, S. Lara, and S. Tlali. "Effects of size and shape on the specific heat, melting entropy and enthalpy of nanomaterials." Journal of Taibah University for Science, **11** (2017) 922.

[17] J. G. Dash "History of the search for continuous melting." Reviews of Modern Physics, **71** (1999) 1737.

[18] Zhu, Y. F., J. S. Lian, and Q. Jiang. "Modeling of the melting point, Debye temperature, thermal expansion coefficient, and the specific heat of nanostructured materials." The Journal of Physical Chemistry C, **113** (2009) 16896.

[19] James H. Rose, John Ferrante, and John R. Smith. "Universal binding energy curves for metals and bimetallic interfaces." Physical Review Letters, **47** (1981) 675.

[20] L. Dongwook et al. "Quantum confinement-induced tunable exciton states in graphene oxide." Scientific Reports, **3** (2013) 2250.

[21] G. Compagnini et al. "Ion beam induced defects in graphene: Raman spectroscopy and DFT calculations." Journal of Molecular Structure, **993** (2011) 506.

[22] C. Thomsen, M. Machón, and S. Bahrs. "Raman spectra and DFT calculations of the vibrational modes of hexahelicene." Solid state communications, **150** (2010) 628.

[23] M. W. Smith et al. "Structural analysis of char by Raman spectroscopy: Improving band assignments through computational calculations from first principles." Carbon, **100** (2016) 678.

[24] F. Tuinstra and J. Lo Koenig. "Raman spectrum of graphite." The Journal of Chemical Physics, **53** (1970) 1126.

[25] Andrea C. Ferrari et al. "Raman spectrum of graphene and graphene layers." Physical Review Letters, **97** (2006) 187401.

[26] R. P. Vidano et al. "Observation of Raman band shifting with excitation wavelength for carbons and graphites." Solid State Communications, **39** (1981) 341.

[27] N.S.R., N.C.W. (2017) Standard Reference Data Act.